Regulatory role of permanent gullies in dissolved nitrogen and phosphorus transport under different rainfall types

Zhuoxin Chen[1,2], Mingming Guo[1], Lixin Wang[1,3,5], Xin Liu[1], Jinshi Jian[2], Qiang Chen[4], Xingyi Zhang[1]

[1] State Key Laboratory of Black Soils Conservation and Utilization, Northeast Institute of Geography and Agroecology, Chinese Academy of Sciences, Harbin, China
[2] State Key Laboratory of Soil and Water Conservation and Desertification Control, Northwest A&F University, Yangling, China
[3] Institute of Soil and Water Conservation, Chinese Academy of Sciences and Ministry of Water Resources, Yangling, China
[4] Harbin Normal University, Harbin, China
[5] University of Chinese Academy of Sciences, Beijing, China

Correspondence to: Mingming Guo (guomingming@iga.ac.cn)

Abstract. Understanding how permanent gullies regulate the transport of dissolved ammonium (NH_4^+), nitrate (NO_3^-), and phosphorus (P) in runoff delivered from agricultural hillslopes under different rainfall types is essential for controlling non-point source pollution in agroecosystems. In this study, we selected two agricultural catchments, each containing a single permanent gully, and monitored runoff at the gully head and the gully outlet during the rainy seasons of 2022 and 2023. Runoff samples were filtered through 0.45 μm membrane filters and analyzed for dissolved NH_4^+, NO_3^-, and P concentrations, and the corresponding nutrient transport fluxes were then calculated. Based on event-scale rainfall characteristics, including rainfall depth, duration, average intensity, maximum 30-min intensity, and erosivity, rainfall events were classified using the k-means method to examine how different rainfall types influenced the role of gullies in the transport of dissolved NH_4^+, NO_3^-, and P. The results showed that: (1) Gullies significantly enhanced runoff generation, contributing 36.1% of total runoff despite occupying only 12.4% of the catchment area. This contribution varied across rainfall types (Type A: frequent, low-depth, low-erosivity; Type B: short-duration, high-intensity; Type C: long-duration, high-erosivity) and was highest under Type A (43.2%) and lowest under Type C (33.8%). (2) Gullies exerted a pronounced dilution effect on dissolved NH_4^+, NO_3^-, and P concentrations, particularly on dissolved NO_3^- (dilution ratio: 0.65). Consequently, the contribution of gullies to dissolved NH_4^+, NO_3^-, and P transport fluxes was lower than that to runoff volume, accounting for 31.4%, 22.4%, and 31.1% of dissolved NH_4^+, NO_3^-, and P transport fluxes at the outlet, respectively. (3) Type C rainfall dominated the transport of dissolved NH_4^+, NO_3^-, and P. Only 10.2% of events contributed over 68% of dissolved NH_4^+, NO_3^-, and P transport fluxes at the catchment scale and markedly increased their transport sensitivity to rainfall compared to Type A and Type B. These sensitivities were also intensified by gullies. These findings highlight the importance of prioritizing permanent gullies and high-erosivity rainfall events in strategies to reduce dissolved nutrient losses from agricultural catchments.

1 Introduction

The transport of nitrogen (N) and phosphorus (P) via agricultural surface runoff poses a major challenge to watershed management, as these nutrients are key contributors to downstream eutrophication (Berretta & Sansalone, 2011; McDowell & Haygarth, 2024; Huo et al., 2025). Dissolved nitrogen (DN) and dissolved phosphorus (DP), which are the most mobile and bioavailable forms, are rapidly transported to aquatic systems during rainfall events, where they can trigger algal blooms due to their high ecological reactivity (Wang et al., 2024; Xiao et al., 2024). Compared to particulate forms, DN and DP respond more quickly to storm-driven hydrological processes and are more easily mobilized along surface flow paths (Berretta & Sansalone, 2011). In agricultural landscapes, these flow paths are often shaped by permanent gullies that act as hydrological conduits linking farmland to downstream water bodies. Gullies are widespread in farmland across China, the United States, and various regions of Europe and Australia (Dube et al., 2020; Shi et al., 2022; Walker et al., 2024; Chen et al., 2025c). However, their role in regulating hydrological processes and dissolved nutrient dynamics under natural rainfall remains insufficiently quantified.

Unlike engineered drainage ditches, these gullies typically lack vegetation cover, experience minimal human intervention, and are often subject to severe erosion (Wang et al., 2019; Kumar Bhattacharya et al., 2024). Such characteristics suggest that gullies function not only as efficient hydrological pathways but also as dynamic regulators of nutrient transport, serving as sources, sinks, or regulators depending on prevailing hydrological conditions (Miller et al., 2016; He et al., 2024). DN and DP, owing to their higher mobility and bioavailability, are more responsive to hydrological processes and land use changes than their particulate forms (Lee et al., 2013). Land use exerts a critical influence on nutrient fluxes: forests, grasslands, and riparian zones often act as nutrient sinks (Miller et al., 2016; Räty et al., 2020), whereas intensively managed croplands, frequently subject to fertilizer misapplication, represent major nutrient sources (Liu et al., 2020; Risal et al., 2020; Wang et al., 2025). In agricultural catchments, gullies predominantly receive runoff from upslope cultivated fields (Zhang et al., 2011), and their sparse vegetation and limited internal nutrient inputs may further modulate nutrient transport processes (Ezzati et al., 2020). Steep gully gradients intensify runoff energy and hydrological connectivity, accelerating sediment transport (Kumar Bhattacharya et al., 2024). Studies have shown that deposited sediments within gullies may be remobilized during rainfall events, releasing dissolved nutrients and thereby posing a potential risk of secondary pollution (Miller et al., 2016; Ezzati et al., 2020; Xu et al., 2022). However, existing studies have mainly focused on nutrient spatial redistribution (Sun et al., 2022; Wang et al., 2026), snowmelt-driven transport (Chen et al., 2024c), or total nitrogen and phosphorus transport associated with gullies (Chen et al., 2025b). By contrast, the influence of permanent gullies on dissolved nutrient transport under natural rainfall conditions remains poorly constrained, which hinders effective nutrient management at the catchment scale.

Moreover, the strength and direction of this regulatory effect are likely to depend on rainfall type. Rainfall characteristics, including depth, intensity, duration, and erosivity, are key drivers of runoff generation, erosion, and nutrient mobility in agricultural landscapes (Wang et al., 2024; Wang et al., 2025). As a result, different rainfall types, ranging from

more frequent low-intensity events to less frequent high-intensity events, may lead to marked variation in nutrient mobilization, transport pathways, delivery processes, and associated environmental risks (Wang et al., 2024; Yang et al., 2024; Wang et al., 2025). For example, nitrate transport pathways have been shown to vary significantly with rainfall characteristics. Under low-intensity rainfall, transport is mainly restricted to near-stream contributing areas, whereas increasing rainfall intensity progressively expands these pathways from riparian zones to hillslopes, leading to complex dynamic changes in the sources and concentrations of nitrate in runoff (Wang et al., 2024). Likewise, both the number of critical source areas for phosphorus transport and the intensity of phosphorus export increase significantly with rainfall intensity (Zhao et al., 2026). Against the backdrop of the ongoing intensification of extreme weather events under global climate change, the influence of heavy storms on nutrient export from agricultural catchments is expected to become even more pronounced (Zhang & Zhang, 2025; Bian et al., 2026). In general, heavy storms are increasingly associated with intense erosion and elevated nutrient loads, often resulting in DN and DP exports that greatly exceed those observed under moderate rainfall (Lei et al., 2026). Conversely, low-intensity rainfall events may favor nutrient dilution or retention due to reduced flow velocities and longer contact times for nutrient exchange (Wang et al., 2025). Disparities in soil properties, vegetation cover, and topography between upslope areas and gullies may further amplify these effects (Miller et al., 2016). Nevertheless, the role of gullies in modulating dissolved nutrient transport under varying rainfall conditions remains insufficiently investigated. This limitation is especially critical in gully-dominated agricultural regions, where rainfall-driven hydrological connectivity may strongly influence nutrient delivery from fertilized hillslopes to downstream waters.

The Mollisols region of Northeast China (MRNC) is a typical example of such a landscape. As a cornerstone of national food security (Chen et al., 2025a), the region depends on intensive agricultural production and substantial fertilizer inputs, which increase the risk of agricultural non-point source pollution (Zhao et al., 2025). At the same time, decades of extensive land development have resulted in widespread gully erosion and land degradation. More than 667,000 permanent gullies have been identified, posing serious threats to agricultural sustainability (Chen et al., 2025c). Earlier studies have explored the influence of rainfall characteristics on gully formation (Tang et al., 2023; Liu et al., 2024), as well as the function of gullies in sediment and nutrient transport during snowmelt events (Su et al., 2024). However, how permanent gullies regulate DN and DP transport under natural rainfall conditions remains poorly understood. This knowledge gap is largely attributed to technical challenges in field-based monitoring, which have constrained a comprehensive understanding of gully-mediated nutrient dynamics and their implications for watershed-scale water quality management in the MRNC.

To address these gaps, this study monitored runoff and associated transport processes of dissolved ammonium (NH_4^+), nitrate (NO_3^-), and phosphorus (P) at both the gully head and gully outlet in two agricultural catchments in the MRNC during natural rainfall events in 2022 and 2023. The specific objectives were to: (1) elucidate the regulatory effect of gullies on runoff, dissolved NH_4^+, NO_3^-, and P transport fluxes; (2) quantify how gully contributions to these transport fluxes vary in response to different rainfall types; and (3) reveal how gullies regulate the response relationship between rainfall and dissolved NH_4^+, NO_3^-, and P transport fluxes. By linking event-based rainfall characteristics with field-monitored runoff and

dissolved nutrient fluxes, this study aims to support targeted mitigation of rainfall-type-dependent dissolved nutrient loss in agricultural catchments.

2 Materials and methods

2.1 Study area

The study area is located in Guangrong Village (47°34′–47°38′ N, 126°81′–126°88′ E), Hailun City, Heilongjiang Province, within the central MRNC (Fig. 1A). The region experiences a continental monsoon climate, with annual precipitation of 300–900 mm during 2000–2022, of which approximately 80.7% falls between June and October, coinciding with the peak period of soil erosion. The mean annual temperature is ~1.5°C (-25.6°C to 26.6°C), with crop sowing typically commencing in mid-April. The terrain comprises gently rolling hills, and the soils are classified as Mollisols (Chernozem) with a silty clay loam texture, 45–60% silt content, and an organic matter content of >3% in the ploughed layer. These conditions support intensive maize and soybean cultivation, but sustained anthropogenic disturbance has caused a ~20% decline in soil fertility. In particular, gully erosion on sloping farmland leads to an annual arable land loss of ~0.097%, with gully density reaching 1.5 km km^{-2} (Chen et al., 2025c).

To assess the morphological characteristics and activity status of the gullies in the region, a comprehensive gully survey was conducted in May 2021 prior to hydrological monitoring. The results revealed that over 90% of farmland gullies were highly active, with average widths and depths of 13.3 m and 3.4 m, respectively. On this basis, two permanent gullies in farmland catchments (F1 and F2) were selected (Fig. 1B–E), as they exhibited similar catchment areas, land use proportions, and typical morphological and topographic features. Each catchment contained only one permanent gully, and both gullies exhibited clear signs of active development. The gully heads were highly susceptible to headward erosion under rainfall-driven runoff. In addition, vegetation cover on the gully slopes was relatively sparse, particularly in the upstream sections of the gullies (Fig. 1F–G). The characteristics of the two catchments and their gullies are described as follows. The F1 and F2 catchments cover 4.3 ha and 3.4 ha, respectively. Farmland is the dominant land use, comprising 83.4% of F1 and 85.5% of F2. The area directly occupied by the gully accounts for 9.6% and 15.2% of the total catchment area in F1 and F2, respectively, with a mean value of 12.4%. In contrast, the upslope drainage area of the gully head (UDGH) accounts for 64.8% and 43.9% of the catchment area in F1 and F2, respectively (mean: 54.3%), and is entirely covered by farmland. Moreover, gully dimensions were consistent with the survey averages: the gully in F1 measured 0.38 ha in area, 242.3 m in length, 17.7 m in width, and 3.8 m in depth, and the gully in F2 measured 0.54 ha, 293.7 m, 18.4 m, and 4.8 m, respectively. Gully slope gradients (F1: 36.2°; F2: 39.5°) were significantly steeper than those of the adjacent farmland slopes (F1: 4.3°; F2: 3.4°). In addition, within the catchments, basal fertilizer was applied at the end of April during ridge formation and sowing using a fertilizer seeder, such that fertilization and sowing were completed simultaneously. The remaining fertilizer was then top-dressed in mid- to late June at the maize jointing stage. Meanwhile, during the rainy season, crop cover on the agricultural upslope areas exceeded 90%, while vegetation cover within the gullies exceeded 70%. It should also be noted that a 2 m-

wide unplanted buffer along the gully bank, maintained for machinery access, was colonized by natural grass cover (Fig. 1F–G). Field monitoring during intense rainfall indicated that these grass strips, together with wheel ruts, effectively diverted lateral runoff downslope along their margins, reducing direct flow into the gullies (Chen et al., 2025b). Therefore, this minor component was excluded when estimating the contribution of the gully to runoff and dissolved NH_4^+, NO_3^-, and P transport fluxes.

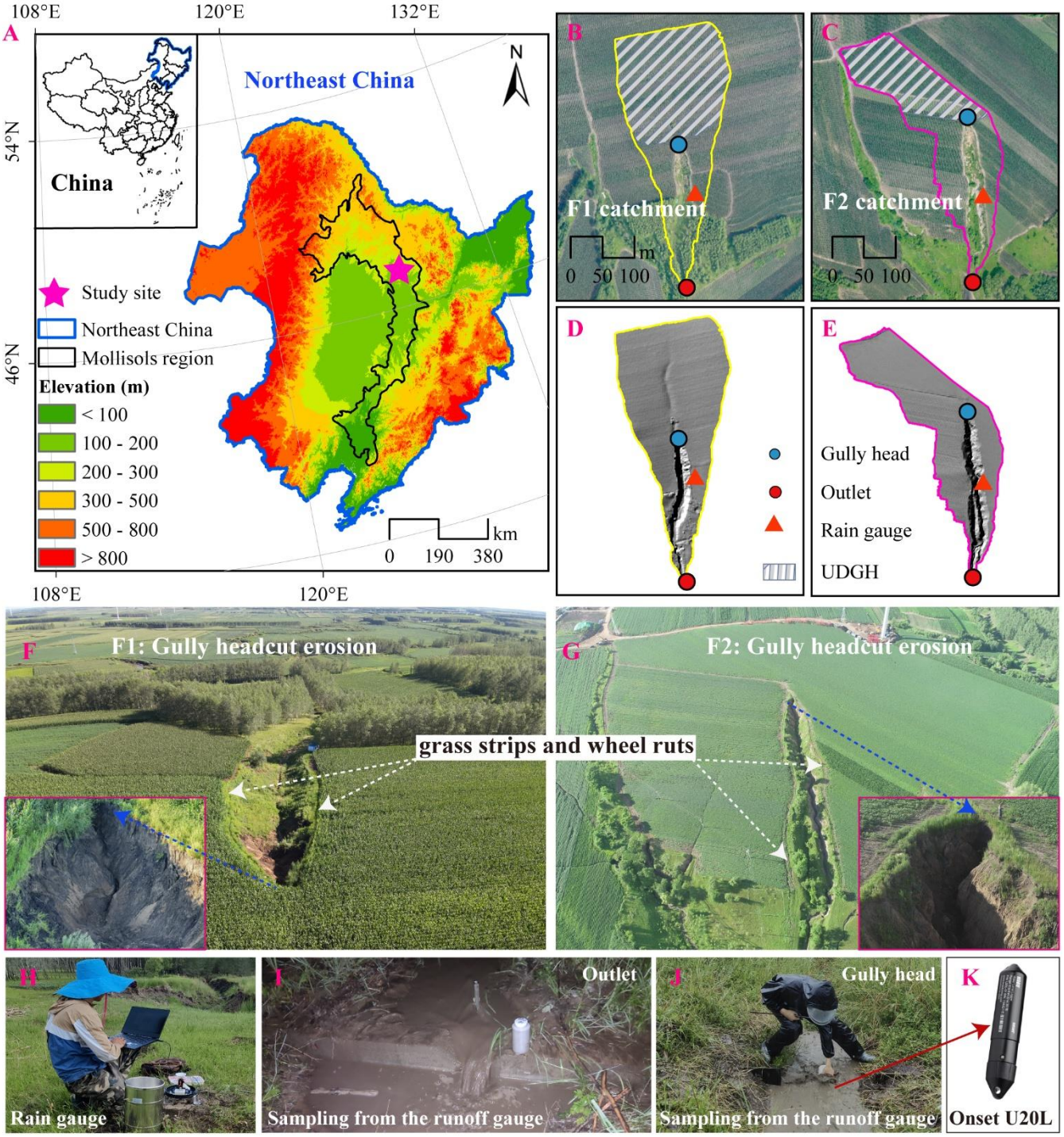

Fig. 1 (A) Location of the study site within the MRNC; (B–C) overview of the two monitored gully-dominated catchments; (D–E) DEM-derived hillshade maps; (F–G) UAV aerial images of the two gullies; (H) rainfall data acquisition; (I–J) runoff sampling at the measuring weirs; and (K) water level monitoring using pressure sensors. UDGH represents the upslope drainage area of the gully head.

2.2 Rainfall data

From June to October in both 2022 and 2023, tipping-bucket rain gauges (Jian Darenke Electronic Technology Co., Ltd., Jinan, China) with a resolution of 0.2 mm were installed in each catchment to characterize rainfall conditions at the catchment scale (Fig. 1B, C, and H). A rainfall event was defined as a continuous precipitation event separated from the next rainfall event by at least 6 h without rainfall; shorter dry intervals were considered part of the same event, whereas longer intervals were treated as separate events. Effective rainfall events were defined as those that generated observable surface runoff at the catchment outlet. Accordingly, only rainfall events associated with observable runoff were included in the subsequent analysis (Chen et al., 2024b). Because the monitored catchments are hillslope systems without baseflow under dry conditions, runoff occurred only in response to rainfall and ceased shortly after rainfall ended. Therefore, the beginning and end of each runoff event were determined by combining field observations with automatic monitoring records at the measuring weirs, with runoff initiation defined as the time when flow was first detected and runoff termination defined as the time when flow ceased. To evaluate the impacts of different rainfall types on dissolved NH_4^+, NO_3^-, and P transport fluxes, five parameters were selected for cluster analysis: rainfall depth, duration, average intensity, maximum 30-min intensity, and rainfall erosivity. The calculation of rainfall erosivity (*RE,* MJ·mm·ha^{-1}·h^{-1}) is shown in Equations (1)–(3):

$$RE = K_e \cdot I_{30} \quad (1)$$

$$K_e = \sum(P_r \cdot E_r) \quad (2)$$

$$E_r = 0.29[1 - 0.72e^{-0.082 i_r t}] \quad (3)$$

In Eq. (1), K_e represents the total kinetic energy of a rainfall event (MJ ha^{-1}), and I_{30} denotes the maximum rainfall intensity in 30 min (mm h^{-1}); In Eq. (2), P_r represents the rainfall amount of segment r (mm); and in Eq. (3), Er denotes the unit kinetic energy during rainfall segments r (MJ ha^{-1} mm^{-1}). Here, r = 1, 2, ..., n refers to the consecutive rainfall segments within a single rainfall event, which were defined according to the temporal variation in recorded rainfall intensity; and i_r is the rainfall intensity during rainfall segment r (mm h^{-1}).

2.3 Runoff monitoring and sample collection

To capture runoff variations during rainfall events, measuring weirs were installed at both the gully head (upslope drainage area of the gully head; UDGH) and the catchment outlet (Fig. 1I–K). HOBO Water Level Probes (Onset Computer Corporation, Bourne, MA, USA) recorded runoff dynamics at 10-minute intervals by measuring pressure differences relative to identical probes placed in the air (Cheng et al., 2023; Chen et al., 2025b). Runoff samples were manually collected during rainfall events at the rising, peak, and recession stages of runoff using 1,000 mL polyethylene bottles. Depending on runoff duration and flow variability, 3–23 runoff samples were collected for each event, with an average of 6 samples per event. After the rising and peak stages had been adequately characterized, sampling intervals were gradually extended during the late runoff stage to ensure full event coverage. All collected samples were immediately delivered to the laboratory for

dissolved NH_4^+, NO_3^-, and P analysis. Notably, no baseflow was observed in either gully during non-rainfall periods; therefore, its potential influence on the runoff process was excluded from consideration.

A subsample was filtered through a 0.45 μm Millipore membrane to obtain the filtrate for nutrient analysis. Concentrations of dissolved NH_4^+, NO_3^-, and P were determined using standard spectrophotometric methods: Nessler's reagent spectrophotometry for NH_4^+, ultraviolet spectrophotometry for NO_3^-, and ammonium molybdate spectrophotometry for dissolved P. The runoff volume for each rainfall event was calculated using the calibrated weir depth-discharge curve and an empirical formula. By integrating high-frequency runoff sampling and dissolved nutrient concentrations, the dissolved nutrient transport flux for each rainfall event was determined (Eq. 4). Specifically, nutrient concentrations measured from discrete runoff samples were assigned to their corresponding sampling intervals, and the event-scale dissolved nutrient transport flux was calculated by summing the products of runoff volume and nutrient concentration across the entire runoff process (Bender et al., 2018). A detailed description of the calculation process can be found in our previous study (Chen et al., 2025b). In addition, after rainfall events were classified, dissolved nutrient transport fluxes were further aggregated within each rainfall type to compare differences in cumulative nutrient transport fluxes among rainfall types.

$$F = \int_{t_1}^{t_2} \frac{Q_t \cdot C}{1000} d_t \quad (4)$$

Where F is the transport flux of dissolved NH_4^+, NO_3^-, and P (kg). Q_t refers to the runoff discharge at time t ($m^3\ h^{-1}$). t_1 and t_2 correspond to the times when runoff begins and ends, respectively (h). C represents the concentrations of dissolved NH_4^+, NO_3^-, and P ($mg\ L^{-1}$).

2.4 Data analysis

Rainfall types were classified using K-means clustering analysis via the R package "cluster" (v.2.1.3). To compare event-scale dissolved nutrient transport fluxes among different rainfall types, data normality and variance homogeneity were first assessed using Shapiro's test and Levene's test, respectively. If these assumptions were met, one-way ANOVA followed by Tukey's HSD test was used to compare dissolved NH_4^+, NO_3^-, and P transport fluxes across rainfall types; otherwise, the Kruskal-Wallis nonparametric test was applied. A statistically significant difference ($P < 0.05$) was interpreted as evidence that rainfall type significantly influenced dissolved nutrient export dynamics. To quantify changes in dissolved NH_4^+, NO_3^-, and P concentrations during transport through the gully, a dilution ratio was calculated for each event as the outlet concentration divided by the corresponding concentration at the gully head. Values lower than 1 indicate dilution during transport through the gully, whereas values greater than 1 indicate enrichment. Correlation analysis was used to examine the relationships between dissolved NH_4^+, NO_3^-, and P transport fluxes and rainfall characteristics. Redundancy analysis (RDA) was employed to explore the individual effects of rainfall, runoff, and dissolved nutrient concentrations on dissolved NH_4^+, NO_3^-, and P transport fluxes. Model significance was assessed using a Monte Carlo permutation test with 999 permutations, and the relative importance of each explanatory variable was then determined through hierarchical partitioning. In addition, to assess the effects of gullies and rainfall types on dissolved NH_4^+, NO_3^-, and P transport fluxes,

the relationships between nutrient transport fluxes and rainfall depth were fitted using either power or linear functions. A significant power function relationship (F=aR^b) was observed between rainfall depth and the transport fluxes of dissolved NH_4^+, NO_3^-, and P, where the coefficient a indicates the sensitivity of nutrient transport fluxes to rainfall (higher values reflect greater mobilization potential) and the exponent b represents the efficiency with which transport fluxes respond to changes in rainfall depth. In the linear function (F=aR+b), parameter a likewise reflects the sensitivity of dissolved NH_4^+, NO_3^-, and P transport fluxes to rainfall depth. All statistical analyses were performed in R (v.4.5.0; R Core Team, Vienna, Austria).

3 Results

3.1 Rainfall characteristics

From June to October of 2022 and 2023, 30 and 29 rainfall events were recorded in F1 and F2, respectively. K-means clustering classified these events into three distinct rainfall types (Table 1). Type A was characterized by low rainfall depth (20.8 mm), moderate duration (8.2 h), moderate intensity (3.9 mm h^{-1}), and low erosivity (71.9 MJ mm ha^{-1} h^{-1}). Type B featured moderate rainfall depth (23.8 mm), short duration (0.9 h), high intensity (28.3 mm h^{-1}), and moderate erosivity (267.4 MJ mm ha^{-1} h^{-1}). Type C exhibited high rainfall depth (79.6 mm), long duration (48.7 h), low intensity (1.7 mm h^{-1}), and the highest erosivity (333.7 MJ mm ha^{-1} h^{-1}). Among these rainfall types, Type A was dominant, occurring 23 times in each catchment, while Types B and C were less frequent (F1: 4 and 3; F2: 3 and 3, respectively). However, the erosivity of Types B and C was 3.6 and 4.3 times higher than that of Type A, respectively (Table 1).

Table 1 Average values of rainfall parameters for the three rainfall types identified in catchments F1 and F2.

Catchments	Rainfall types	Sample sizes	P (mm)	D (h)	I_{mean} (mm h^{-1})	I_{30} (mm h^{-1})	RE (MJ mm ha^{-1} h^{-1})
F1	A	23	21.5	8.8	3.4	17.1	84.5
	B	4	24.5	0.9	30.3	46.1	334.2
	C	3	82.5	49.3	1.8	20.8	515.7
F2	A	23	20.1	7.6	4.5	13.7	59.3
	B	3	23.1	1.0	26.2	32.9	200.6
	C	3	76.7	48.1	1.6	10.5	151.6

Note: F1 and F2 represent the two monitored catchments, respectively. Sample size indicates the number of rainfall events included in each rainfall type. Abbreviations: P, rainfall depth; D, rainfall duration; I_{mean}, mean rainfall intensity; I_{30}, maximum 30-min rainfall intensity; and RE, rainfall erosivity.

3.2 The role of gullies in regulating runoff

During Type C rainfall, cumulative runoff volume in the UDGH was 3.9 and 21.0 times higher than that under Types A and B, respectively, based on the mean values of the F1 and F2 catchments (Fig. 2A–B). At the outlet, cumulative runoff under Type C was 3.3 times higher than that under Type A and 19.0 times higher than that under Type B. On average, Type C rainfall generated significantly more runoff than Types A and B at both locations ($P < 0.05$) (Fig. 2A–B). Specifically, the average runoff volume in the UDGH during Type C was 29.8 and 24.5 times greater than that under Types A and B, respectively, while at the outlet, it was 25.6 and 22.1 times higher than that under Types A and B, respectively (Fig. 2A–B). Although Type B produced more runoff than Type A, the difference was not statistically significant ($P > 0.05$) (Fig. 2A–B).

Gullies accounted for only 12.4% of the catchment area but contributed an average of 36.1% of total runoff (based on the mean value of the F1 and F2 catchments) (Fig. 2C–D). This contribution varied with rainfall type, with the highest value observed under Type A (43.2%), followed by Type B (40.1%), and the lowest value under Type C (33.8%) (Fig. 2C–D).

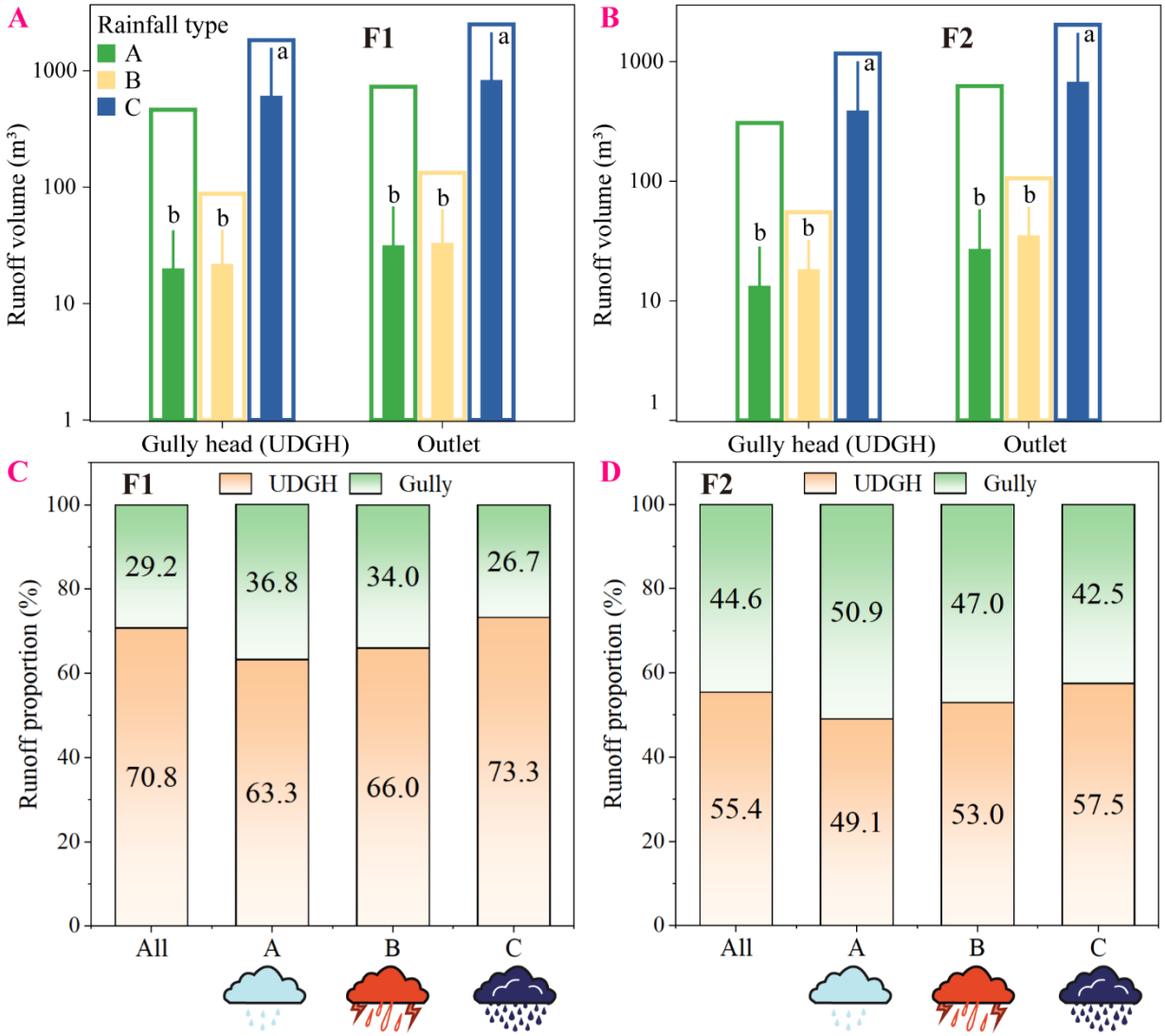

Fig. 2 (A, F1 catchment; B, F2 catchment) Cumulative and event-scale runoff volumes from the UDGH and the gully under different rainfall types. (C, F1 catchment; D, F2 catchment) Contribution of the UDGH and the gully to total runoff under different rainfall types. Note: Bars without fill represent cumulative runoff volume under different rainfall types, whereas embedded bars with fill represent the average runoff volume for individual rainfall events, and different lowercase letters represent significant differences in runoff volume between different rainfall types (A–B). Abbreviation: UDGH represents the upslope drainage area of the gully head.

3.3 Transport of dissolved NH_4^+, NO_3^- and P mediated by gullies

3.3.1 Concentrations of dissolved NH_4^+, NO_3^- and P

Dissolved NH_4^+, NO_3^-, and P concentrations measured at the outlet were consistently lower than those observed at the gully head (Fig. 3). On average, the dilution ratios were 0.77 for dissolved NH_4^+, 0.65 for NO_3^-, and 0.87 for P. These values indicated that the gully exerted a stronger dilution effect on NO_3^- than on NH_4^+ or P (Fig. 3).

The effect of the gully on dissolved NH_4^+, NO_3^-, and P concentrations also varied with rainfall type (Fig. 4). On average, the dissolved NH_4^+ concentrations at the gully head were 1.33, 1.24, and 1.21 times higher than those at the outlet under rainfall Types A, B, and C, respectively (Fig. 4A and D). For dissolved NO_3^-, the corresponding ratios were 1.61, 1.58, and 1.21 (Fig. 4B and E). For DP, the ratios were 1.19, 0.94, and 1.21 (Fig. 4C and F). These results suggested that, under rainfall Types A and B, the gully intensified the concentration gradient of NH_4^+ and NO_3^- between the gully head and the outlet. In contrast, the pattern for DP appeared more variable: dilution occurred under Types A (particularly in catchment F1) and C (particularly in catchment F2), whereas an increase was observed in catchment F1 and a slight increase in catchment F2 under Type B.

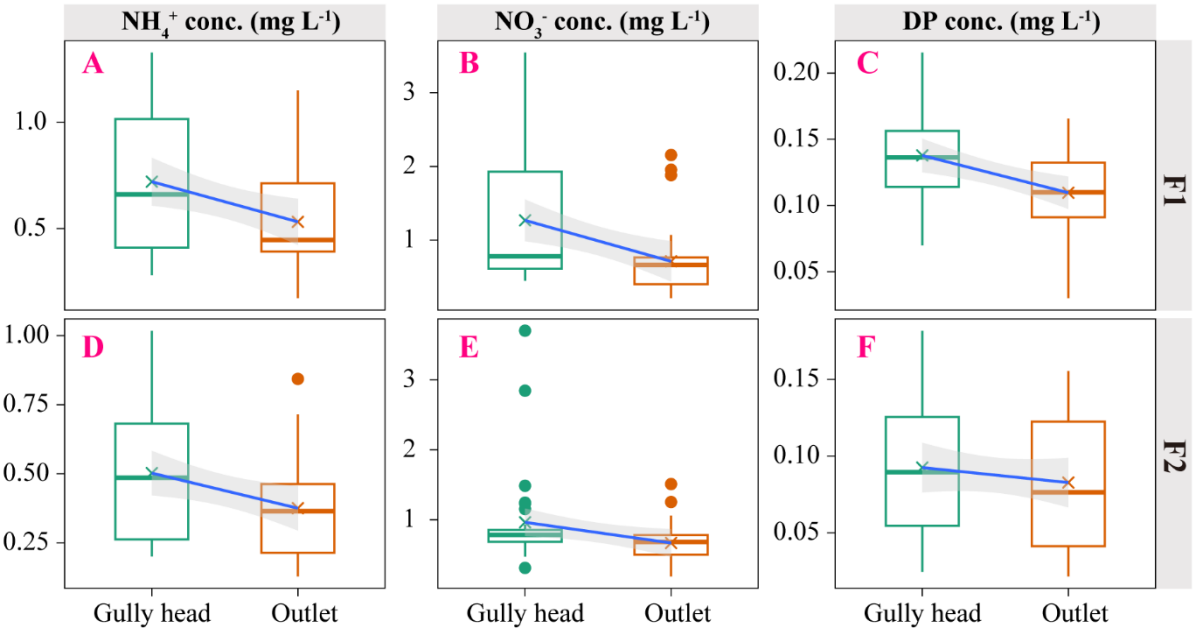

Fig. 3 Comparison of dissolved NH_4^+, NO_3^-, and P concentrations between the gully head and the outlet. (A–C) F1 catchment; (D–F) F2 catchment.

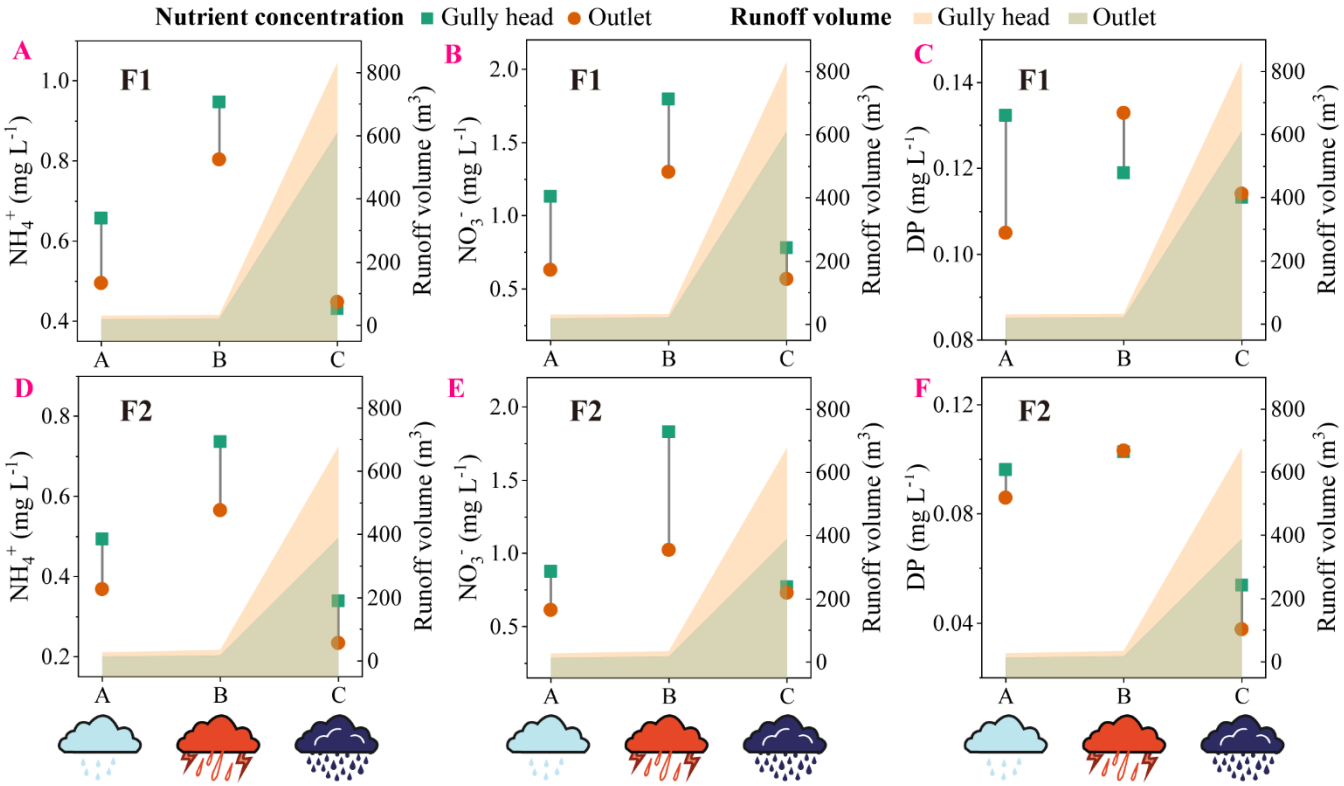

Fig. 4 Dissolved NH_4^+, NO_3^-, and P concentrations under different rainfall types. (A–C) F1 catchment; (D–F) F2 catchment. Note: The length of the lines connecting different points represents the concentration difference between the gully head and the outlet; longer lines indicate larger differences. The colored shaded areas represent the variation in mean runoff volume under different rainfall types at the gully head and the outlet.

3.3.2 Transport fluxes of dissolved NH_4^+, NO_3^- and P

When rainfall types were not differentiated, gullies accounted for 31.4%, 22.4%, and 31.1% of the total dissolved NH_4^+, NO_3^-, and P transport fluxes at the catchment scale, respectively (Fig. 5). Moreover, rainfall type had a significant impact on dissolved nutrient transport. Although Type C rainfall accounted for only 10.2% of all events, it contributed 68.2%, 73.8%, and 71.8% of the total dissolved NH_4^+, NO_3^-, and P transport fluxes at the outlet, respectively (Fig. 6). Meanwhile, the influence of the gully on the transport fluxes of dissolved NH_4^+, NO_3^-, and P in the catchment also depended on rainfall type. On average, the gully accounted for 27.1%, 15.3%, and 34.5% of dissolved NH_4^+ transport fluxes under Types A, B, and C (Fig. 6A and D), respectively, and for 24.8%, 8.0%, and 23.2% of dissolved NO_3^- transport fluxes, respectively (Fig. 6B and E). These results indicate that the gully exerted the strongest reduction in NH_4^+ and NO_3^- fluxes under Type B rainfall and the weakest under Type C. In contrast, gully contributions to DP transport were 22.7%, 40.9%, and 33.1% under Types A, B, and C, respectively, suggesting a reduced regulatory effect during Type B events and an enhanced effect during Type A (Fig. 6C and F).

At the event scale, transport fluxes of dissolved NH_4^+, NO_3^-, and P were significantly higher under Type C rainfall compared to Types A and B ($P < 0.05$). Although the fluxes under Type B exceeded those of Type A, the differences were not statistically significant ($P > 0.05$) (Fig. 7). Specifically, at the gully head (UDGH), NH_4^+ transport fluxes under Type C rainfall were 3.1 and 7.6 times higher than those under Types A and B, respectively; NO_3^- transport fluxes were 3.3 and 9.7 times higher than those under under Types A and B, respectively; and DP transport fluxes were 2.5 and 10.1 times higher than those under Types A and B, respectively (Fig. 7). At the outlet, NH_4^+ transport fluxes under Type C rainfall were 4.3-fold higher than those under Type A and 22.2-fold higher than those under Type B. The corresponding multiples were 2.7 and 57.0 for NO_3^- and 5.8 and 7.2 for DP (Fig. 7).

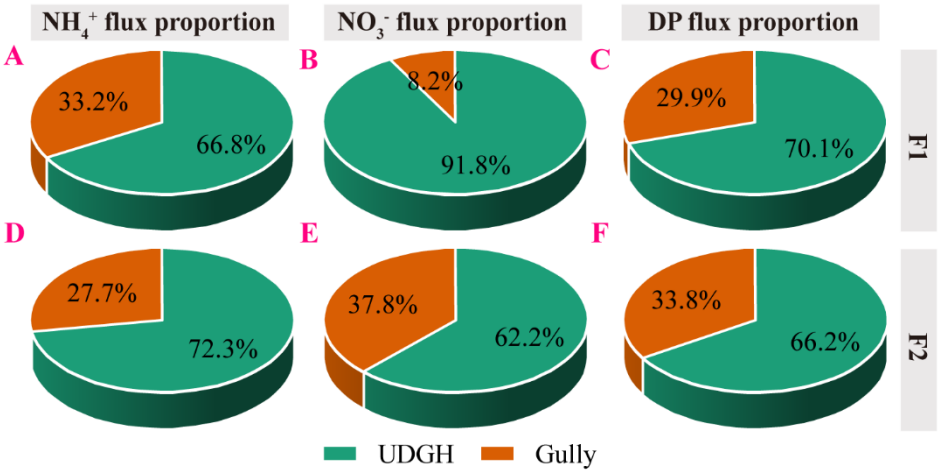

Fig. 5 Contributions of the UDGH and the gully to dissolved NH_4^+, NO_3^-, and P transport fluxes. (A–C) F1 catchment; (D–F) F2 catchment. Abbreviation: UDGH represents the upslope drainage area of the gully head.

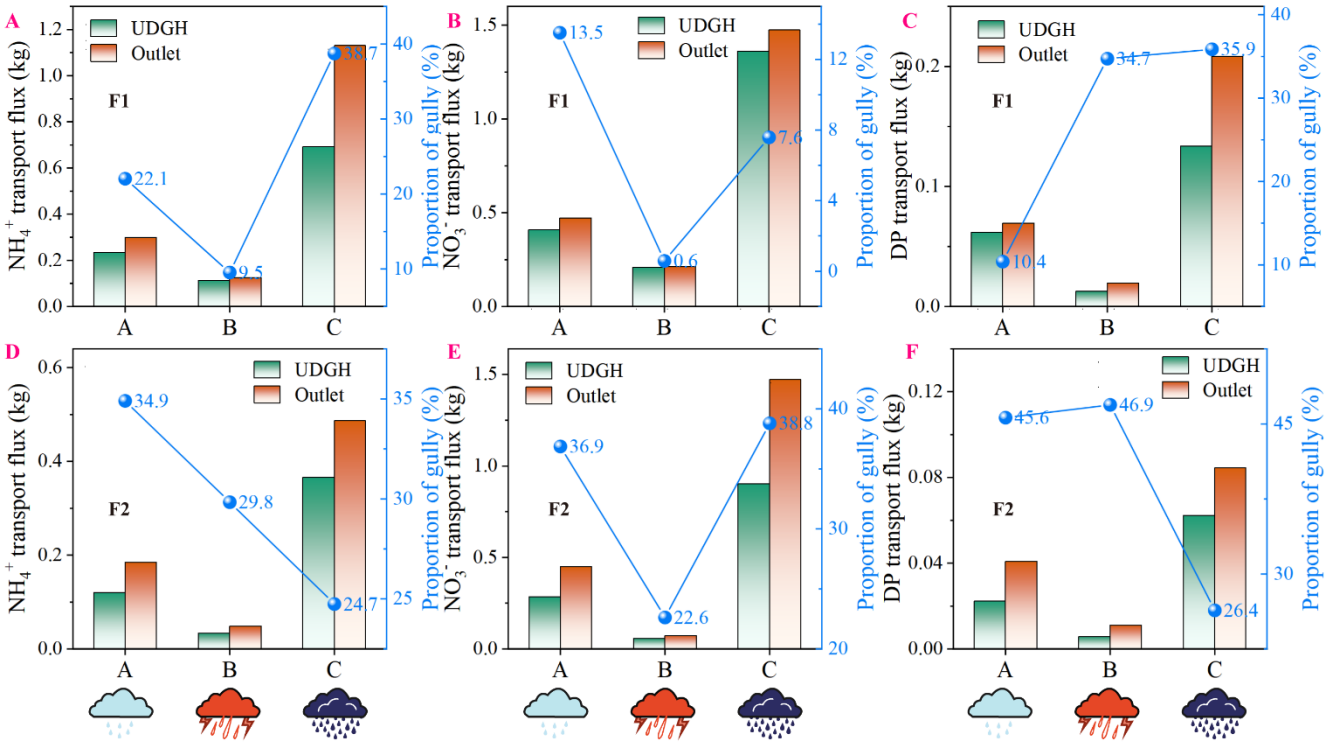

290 **Fig. 6 The left y-axis represents the cumulative transport fluxes of dissolved NH_4^+, NO_3^-, and P under different rainfall types, presented as bar charts. The right y-axis represents the corresponding gully contribution, illustrated by a dotted line. (A–C) F1 catchment; (D–F) F2 catchment. Abbreviation: UDGH represents the upslope drainage area of the gully head.**

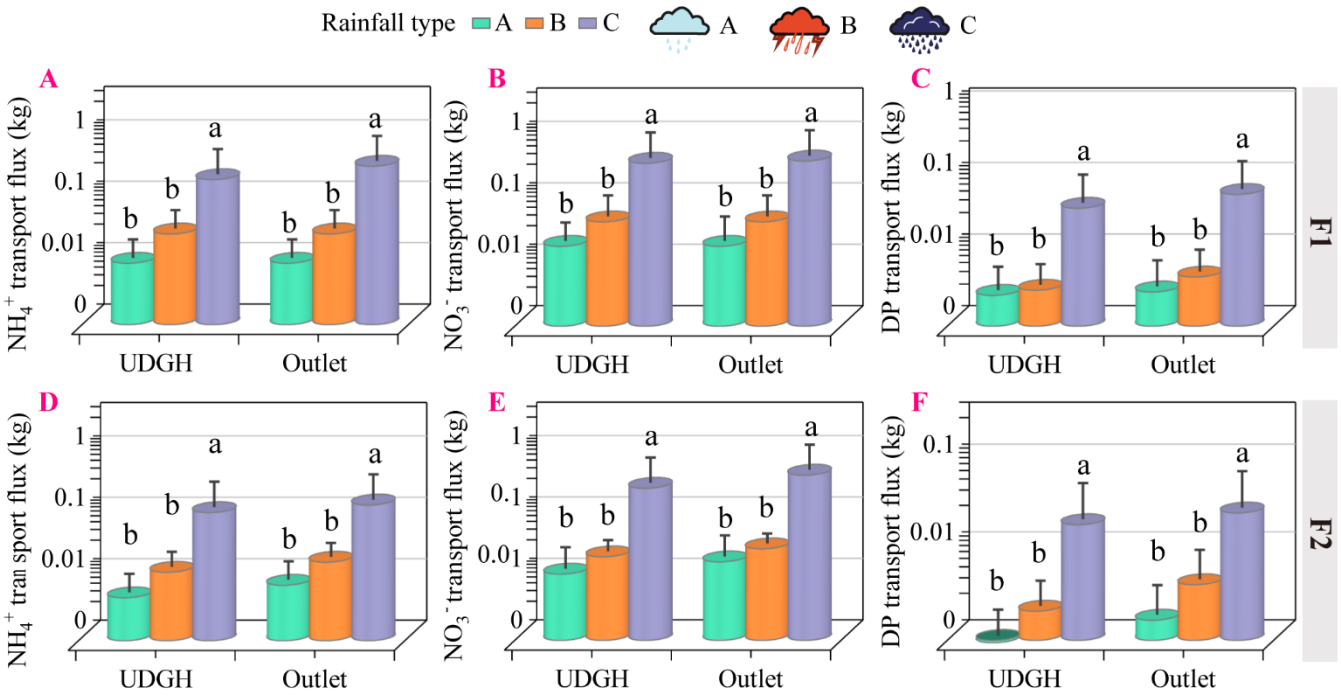

Fig. 7 Effects of different rainfall types on the mean event-scale transport fluxes of dissolved NH_4^+, NO_3^-, and P. (A–C) F1 catchment; (D–F) F2 catchment. Abbreviation: UDGH represents the upslope drainage area of the gully head.

3.4 Rainfall response of dissolved NH_4^+, NO_3^-, and P transport in gully-dominant catchments

At both the gully head and the outlet, rainfall depth was the factor most strongly correlated with runoff volume and dissolved NH_4^+, NO_3^-, and P transport fluxes, followed by rainfall erosivity (Fig. S1). Moreover, redundancy analysis indicated that dissolved NH_4^+, NO_3^-, and P transport fluxes were primarily influenced by runoff volume, rainfall depth, and rainfall type, which ranked as the three most important factors, while their correlations with the corresponding concentrations were not significant. This indicates that dissolved NH_4^+, NO_3^-, and P transport fluxes were influenced more strongly by runoff and rainfall than by concentration (Fig. S2).

The power-law relationships between dissolved NH_4^+, NO_3^-, and P transport fluxes and rainfall depth revealed the regulatory role of gullies in modulating transport sensitivity (Fig. 8). The results showed that the gully significantly increased the sensitivity coefficient (a) for dissolved NH_4^+, NO_3^-, and P transport fluxes, with increases of 3.04, 1.71, and 2.84 times, respectively. However, gullies also reduced the overall transport efficiency (parameter b), by 4.8%, 2.0%, and 19.5% for dissolved NH_4^+, NO_3^-, and P, respectively (Fig. 8). Among the different rainfall types, Type C rainfall markedly enhanced the sensitivity of dissolved NH_4^+, NO_3^-, and P fluxes compared to Types A and B (Fig. 9). Furthermore, within the same rainfall category, comparison of the slope values of the linear relationships between the gully head and the outlet showed that the presence of the gully amplified the rainfall sensitivity of dissolved NH_4^+, NO_3^-, and P transport at the catchment outlet (Fig. 9).

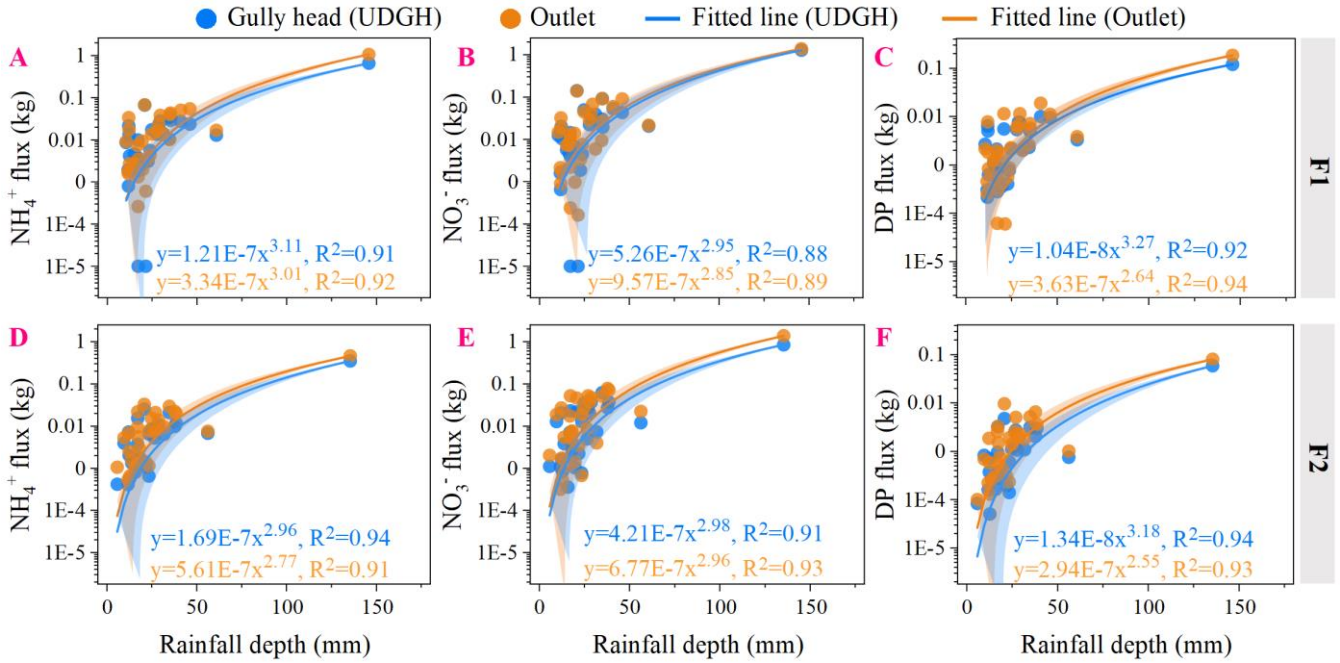

315 **Fig. 8 Differences in the response of dissolved NH_4^+, NO_3^-, and P transport fluxes to rainfall depth between the gully head and the outlet. Solid lines indicate the fitted regression lines. The orange and blue shaded bands indicate the 95% confidence intervals of the fitted lines for the outlet and gully head, respectively. (A–C) F1 catchment; (D–F) F2 catchment. Abbreviation: UDGH represents the upslope drainage area of the gully head.**

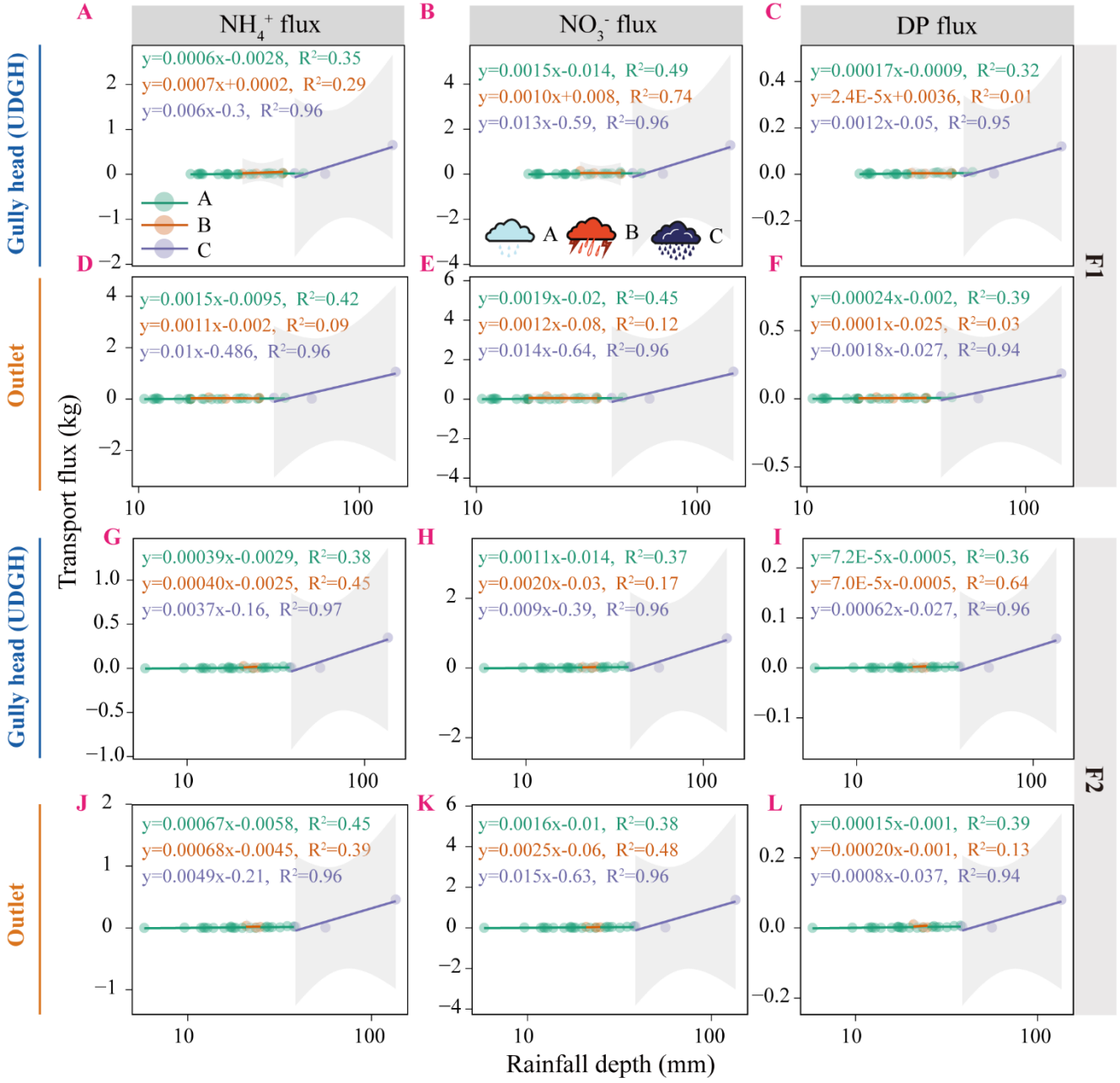

320 **Fig. 9 Differences in the response of dissolved NH_4^+, NO_3^-, and P transport fluxes to rainfall depth under different rainfall types. Solid lines indicate the fitted regression lines. The gray shaded bands indicate the 95% confidence intervals of the fitted lines.**

4 Discussion

4.1 Regulatory effect of gullies on the runoff and associated dissolved NH_4^+, NO_3^-, and P transport

Our findings indicated that, although gullies occupied only 12.4% of the catchment area, they contributed 36.1% of the total runoff, highlighting their promotive effect on runoff generation (Fig. 2). Compared with the gently sloping farmland covered by dense crops during the rainy season (Section 2.1), the steep topography and relatively sparse vegetation of the gullies provided favorable conditions for runoff generation and concentration, which is consistent with previous studies (Chen et al., 2025a; Zhang & Zhang, 2025). These studies showed that, compared with bare land, crop-covered slopes can reduce runoff by 55.8%–92.2% (Chen et al., 2025a), and that the runoff coefficient under vegetation cover is only about 10% of that on bare land (Zhang & Zhang, 2025). This effect is mainly related to rainfall interception by vegetation (Zhang et al., 2025), while steeper gully slopes further promote flow concentration (Zhang & Zhang, 2025; Xu et al., 2026). Together, these results suggest that gullies act as efficient hydrological connectors, rapidly transferring water from upslope farmland to the catchment outlet, which agrees with previous studies (Hou et al., 2022; Chen et al., 2024b; Chen et al., 2025b). Notably, gullies also showed a clear dilution effect on dissolved nutrients, especially NO_3^-, for which the average concentration ratio between the outlet and the gully head was 0.65 (Fig. 3). This pronounced reduction in runoff NO_3^- concentration may have resulted from the formation of ponded, anaerobic, or reducing microenvironments in locally flat sections of the gully bed, where denitrifying microorganisms could convert NO_3^- into gaseous nitrogen, thereby significantly lowering its concentration (He et al., 2026). Furthermore, runoff NO_3^-, as a highly mobile anion, is not readily adsorbed by sediments and tends to remain dissolved in gully water. As runoff accumulated, NO_3^- was more prone to dilution than retention (Wang et al., 2024; Zhao et al., 2025). In contrast, NH_4^+, as a positively charged ion, is more likely than NO_3^- to be adsorbed onto soil colloids, retained through cation exchange, and temporarily stored in sediments on the gully bed (Zhao et al., 2025). Therefore, the observed reduction in NH_4^+ concentrations may have been more the result of physical retention than dilution (Wang et al., 2024). Unlike DN, DP does not undergo gaseous transformation and is primarily governed by adsorption processes (Liu et al., 2020; Yang et al., 2024). Its response of DP was therefore more variable, likely because DP concentrations reflected not only runoff transport, but also interactions at the sediment-water interface within the gully (Bender et al., 2018). Our previous results showed that phosphorus concentrations in gully soils and sediments were significantly lower than those on adjacent farmland slopes (Chen et al., 2024c; Chen et al., 2025b; Wang et al., 2026). This pattern suggests that the equilibrium phosphorus concentration in gully sediments was lower than that in runoff water, which may favor phosphate release from sediments, especially under anoxic conditions (Bender et al., 2018). Interestingly, while gullies generally reduced the concentrations of dissolved NH_4^+, NO_3^-, and P from upslope runoff, they also amplified the sensitivity of transport fluxes to runoff (Fig. 8). This indicates that runoff volume, rather than concentration, primarily governed dissolved NH_4^+, NO_3^-, and P transport (Fig. S2). Once runoff connectivity was established, the increase in water volume outweighed the decrease in concentration. Therefore, managing runoff pathways within catchments may be important for reducing dissolved nutrient transport fluxes.

4.2 Rainfall type-dependent gully effects on the transport of runoff and associated dissolved NH_4^+, NO_3^-, and P

This study classified rainfall events using five rainfall parameters to examine how rainfall type affects runoff and dissolved N and P transport fluxes in gully-dominated catchments. This raises an important question: how do the hillslope and gully differ in their hydrological responses under different rainfall types? Our results showed that the runoff contribution of gullies was highest under Type A rainfall (43.2%), followed by Type B (40.1%), and lowest under Type C (33.8%) (Fig. 2C–D). This pattern indicates clear differences in flow-path connectivity between hillslopes and gullies among rainfall types. Previous studies have shown that intense rainfall can activate surface hydrological connectivity through saturation-excess runoff and near-surface lateral flow, thereby connecting more distant potential runoff pathways and allowing runoff from remote hillslopes to participate in the hydrological process (Winter et al., 2022; Bian et al., 2026; Lei et al., 2026). This may explain why hillslope runoff contributed more, whereas gully runoff contributed less, under Type B rainfall with higher intensity and Type C rainfall with greater erosivity (i.e., extreme rainfall events). Different hydrological response patterns are likely to create different conditions for nutrient transport (Winter et al., 2022). In this study, concentrations of dissolved NH_4^+, NO_3^-, and P were significantly higher during the relatively light rainfall events of Types A and B than during the extreme rainfall events of Type C (Fig. 4). A similar pattern has been observed in Southwest China, where nutrient concentrations in runoff decreased with increasing rainfall following straw return practices on sloping farmland (Zhang et al., 2024; Feng et al., 2025). In contrast, monitoring in micro-catchments comprising paddy fields and drylands found that peak concentrations of dissolved NH_4^+ and NO_3^- followed the order of heavy rainstorm > rainstorm > moderate rain (Zhang et al., 2011). In the Jinglin River watershed of the Three Gorges Reservoir area, rainfall intensity was also found to enhance DP concentrations (Chen et al., 2024a), which differs from our results, where DP concentrations were lowest during extreme rainfall events (Fig. 4). As discussed in Section 4.1, the mechanisms driving DN and DP transport differ. Under varying rainfall conditions, the heterogeneity in gully soil, topography, and vegetation may intensify these differences (Wenng et al., 2020; Winter et al., 2022), leading to inconsistent patterns of nutrient concentrations across rainfall types (Feng et al., 2025). In contrast to concentration, nutrient transport fluxes showed a more consistent pattern (Zhao et al., 2026). Extreme storms produced much greater dissolved nutrient fluxes than Types A and B (Fig. 6; Fig. 7), indicating that hydrological forcing, rather than by concentration alone, mainly drove nutrient export during these events (Zhang & Zhang, 2025). At the plot scale in a potato-maize-sweet potato rotation system, dissolved NH_4^+, NO_3^-, and P transport fluxes during intense storm events were 613.8%, 220.5%, and 268.0% higher, respectively, than those during moderate rainfall events (Feng et al., 2025). At the catchment scale, monitoring of 11 agricultural catchments in Canada showed that only three extreme storm events per year contributed 14%–44% of annual dissolved P flux (Ross et al., 2022). These findings help highlight why a small proportion of rainfall events accounted for most dissolved nutrient transport fluxes at the catchment scale (Chen et al., 2018). In addition, the sensitivity of dissolved nutrient fluxes clearly differed among rainfall types. The power-law coefficient a and the slope of the linear relationship with rainfall depth reflected the vulnerability of dissolved nutrient transport to rainfall forcing (Fig. 8). Our results showed that this sensitivity increased markedly under extreme rainfall and was further amplified

by the presence of gullies (Fig. 8; Fig. 9). From a practical perspective, nutrient management in gully-dominated catchments should pay particular attention to low-frequency but high-impact storm events, because a single extreme storm may generate dissolved nutrient transport fluxes comparable to those from several ordinary rainfall events combined (Bian et al., 2026).

4.3 Implications for agricultural catchment management, study limitations, and future research

Compared with artificial drainage ditches, natural gullies are more dynamic because they have active headcut erosion, irregular morphology, steeper slopes, and stronger sediment interactions (Kumar Bhattacharya et al., 2024; Su et al., 2024; Chen et al., 2025b). This highlights the need to treat gullies as distinct geomorphic units rather than simply as natural drainage ditches. This study demonstrates that under natural rainfall conditions, gullies in agricultural catchments play a dual role. They can reduce dissolved nutrient concentrations through dilution or retention, but they can also enhance dissolved nutrient export by increasing runoff connectivity and transport efficiency. These findings provide important guidance for developing best management practices (BMPs) in gully-dominated catchments. The sharp increase in dissolved N and P fluxes during extreme rainfall events was mainly associated with enhanced surface hydrological connectivity. Therefore, a key management priority is to disrupt rapid flow connectivity during heavy storms and improve water and nutrient retention within the catchment. On agricultural upslopes, conservation tillage has been shown to increase water storage, improve surface roughness, and lengthen runoff pathways (Bayad et al., 2022; Chen et al., 2025a; Cui et al., 2025; Feng et al., 2025). In addition, microtopographic modifications such as terracing can effectively intercept runoff and slow surface flow connectivity on hillslopes (Wang et al., 2023; Wu et al., 2025). Because fertilization replenishes nutrient stocks in surface soils, low fertilizer-use efficiency may further aggravate water-quality deterioration, especially in intensively cultivated catchments exposed to frequent storms. Synchronizing fertilizer application with forecast rainfall patterns and using organic fertilizers and slow-release fertilizers may help improve crop nutrient uptake and reduce storm-driven non-point source pollution (Liu et al., 2020; Wenng et al., 2020). Within gullies, increasing vegetation cover on gully slopes and establishing buffer strips along gully margins may be especially important for slowing and weakening rapid surface runoff connectivity during major storms (Krzeminska et al., 2023). In addition, planting nutrient-intercepting vegetation or constructing small wetlands in the middle and lower parts of gullies can reduce pollutant loads and improve surface water quality (Krzeminska et al., 2023). Although these measures provide a practical basis for promoting sustainable agriculture and protecting water quality in the Mollisols region, their implementation still needs to be adjusted to local topography, land use, and rainfall conditions (Wenng et al., 2020).

This study also has several limitations. First, although the catchments were small, rainfall in each catchment was characterized using only one rain gauge, and thus spatial heterogeneity in rainfall within the catchment could not be resolved. Second, although extreme rainfall events were captured during the two-year monitoring period, climate change is expected to alter the frequency and intensity of such events. Longer-term monitoring is therefore needed to test whether the observed patterns remain valid across broader temporal scales and under future climate conditions. Third, a small amount of runoff from the gully banks could not be directly quantified. Although field observations suggested that this component was minor

because grass cover and wheel ruts along the gully margins reduced direct flow into the gully, its contribution may still have led to a slight overestimation of the gully effect. These limitations should be considered when interpreting the results and planning future studies. Future work should further examine how gully morphology, vegetation recovery, and sediment deposition interact with rainfall extremes to regulate dissolved nutrient export. Long-term monitoring across more catchments is also needed to determine whether the patterns observed here are consistent across different gully sizes, developmental stages, and land-use settings. In addition, combining field monitoring with tracer techniques or process-based modeling could help disentangle the relative contributions of hydrological dilution, sediment retention, and in-channel biogeochemical transformation to dissolved nutrient dynamics.

5 Conclusions

Gullies markedly amplified catchment runoff generation, but this effect decreased as the rainfall gradient increased. After runoff entered the gullies, notable dilution of dissolved NH_4^+, NO_3^-, and P concentrations occurred, with the strongest effect observed for NO_3^-. High-erosivity rainfall events (10.2% of total events, Type C rainfall) dominated dissolved nutrient transport, accounting for 68.2%, 73.8%, and 71.8% of total NH_4^+, NO_3^-, and P fluxes, respectively. Gullies enhanced the sensitivity of dissolved NH_4^+, NO_3^-, and P transport to rainfall, with the strongest effect occurring under Type C events. In summary, the developing gullies function not only as hydrological conduits linking upslope farmland with downstream water bodies but also play a regulatory role in dissolved N and P transport under variable rainfall types. These findings enhance our understanding of non-point source pollution processes under different rainfall types and provide a basis for targeted gully management in agricultural landscapes.

Data availability

Data will be made available upon request (guomingming@iga.ac.cn).

Author contributions

Z.C., M.G., and X.Z. conceived and designed the study. Z.C. prepared the initial manuscript, and M.G. and J.J. contributed to manuscript revision. Z.C., M.G., L.W., X.L., and Q.C. were deeply involved in data collection and discussions on experimental design. Z.C., M.G., and X.Z. provided financial support for the research.

Financial support

This study was supported by the Strategic Priority Research Program of the Chinese Academy of Sciences (XDA28010200), State Key Laboratory of Soil and Water Conservation and Desertification Control, Northwest A&F

University (Z2010025001-KJ2513), Young Scientist Group Project of Northeast Institute of Geography and Agroecology, Chinese Academy of Sciences (2023QNXZ03), and China Postdoctoral Science Foundation (2025M781861).

Competing interests

The authors declare that they have no conflict of interest.

References

Bayad, M., Chau, H.W., Trolove, S., et al. Surface runoff and losses of phosphorus from hydrophobic pastoral soils. *Agriculture, Ecosystems & Environment*, *324*, 107690. doi: 10.1016/j.agee.2021.107690, 2022.

Bender, M.A., dos Santos, D.R., Tiecher, T., et al. Phosphorus dynamics during storm events in a subtropical rural catchment in southern Brazil. *Agriculture, Ecosystems & Environment*, *261*, 93-102. doi: 10.1016/j.agee.2018.04.004, 2018.

Berretta, C., and Sansalone, J. Speciation and Transport of Phosphorus in Source Area Rainfall–Runoff. *Water, Air, & Soil Pollution*, *222*(1-4), 351-365. doi: 10.1007/s11270-011-0829-2, 2011.

Bian, Z., Pan, S., Sun, G., et al. Extreme precipitation reshapes nutrient flows and balance in North America's largest river basin. *Science Advances*, *12*(12), eaea3260. doi: 10.1126/sciadv.aea3260, 2026.

Chen, H., Zhang, X., Abla, M., et al. Effects of vegetation and rainfall types on surface runoff and soil erosion on steep slopes on the Loess Plateau, China. *Catena*, *170*, 141-149. doi: 10.1016/j.catena.2018.06.006, 2018.

Chen, L., Guo, C., Zhu, K., et al. Size-dependent of phosphorus loss and migration driven by rainfall: Evidences from observation and stochastic simulation. *Agriculture, Ecosystems & Environment*, *375*, 109220. doi: 10.1016/j.agee.2024.109220, 2024a.

Chen, Q., Zhang, J., Guo, M., et al. Comparison of the effects of five long-term land use and management practices on runoff, soil erosion, and nutrient loss under natural rainfall in the Mollisol region of Northeast China. *Earth Surface Processes and Landforms*, *49*(5), 1606-1620. doi: 10.1002/esp.5789, 2024b.

Chen, Z., Guo, M., Chen, Y., et al. Utilizing an 11-year runoff plot dataset to evaluate the regulation of six land management practices on runoff and sediment on Mollisols slopes and the applicability of the WEPP model. *Soil and Tillage Research*, *252*, 106601. doi: 10.1016/j.still.2025.106601, 2025a.

Chen, Z., Guo, M., Liu, X., et al. Gully transforms the loss pattern of runoff, sediment, nitrogen, and phosphorus in agricultural catchment of Northeast China. *Journal of Hydrology*, *660*, 133503. doi: 10.1016/j.jhydrol.2025.133503, 2025b.

Chen, Z., Guo, M., Zhou, P., et al. Gully regulates snowmelt runoff, sediment and nutrient loss processes in Mollisols region of Northeast China. *Science of The Total Environment*, *940*, 173614. doi: 10.1016/j.scitotenv.2024.173614, 2024c.

Chen, Z., Song, Q., Guo, M., et al. Morphological characteristics of permanent gullies and their relationship with topography in two typical agro-geomorphic regions of Northeast China. *Earth Surface Processes and Landforms*, *50*(1), e6044. doi: 10.1002/esp.6044, 2025c.

Cheng, Z., Zhang, J., Yu, B., et al. Stormflow response and "Effective" hydraulic conductivity of a degraded tropical imperata grassland catchment as evaluated with two infiltration models. *Water Resources Research*, *59*(5), e2022WR033625. doi: 10.1029/2022wr033625, 2023.

Cui, H., Hou, S.-N., Wang, X.-Y., et al. Organic fertilizer-mediated cultivated land conservation and pollution source control in agricultural ecosystem, Northeast China. *Environmental Technology & Innovation*, *37*, 103945. doi: 10.1016/j.eti.2024.103945, 2025.

Dube, H.B., Mutema, M., Muchaonyerwa, P., et al. A global analysis of the morphology of linear erosion features. *Catena*, *190*, 104542. doi: 10.1016/j.catena.2020.104542, 2020.

Ezzati, G., Fenton, O., Healy, M.G., et al. Impact of P inputs on source-sink P dynamics of sediment along an agricultural ditch network. *Journal of Environmental Management*, *257*, 109988. doi: 10.1016/j.jenvman.2019.109988, 2020.

Feng, M., Xu, Q., Li, T., et al. Combined chemical fertilizers and straw return reduce runoff and N and P losses in sloping croplands Evidence from a 3-year field trial under natural rainfall events. *Agriculture, Ecosystems & Environment*, *392*,

109768. doi: 10.1016/j.agee.2025.109768, 2025.
He, D., Xie, X., Liu, T., et al. Fast migrations of nitrogen and phosphorus are driven by microorganism in freshwater lake sediments. *Journal of Soils & Sediments*, *24*(3), 1391-1401. doi: 10.1007/s11368-024-03728-7, 2024.
He, X., Yan, Z., Wang, S., et al. Revealing microbial pathways of N2O production in agricultural ditches. *Water Res*, *288*(Pt B), 124732. doi: 10.1016/j.watres.2025.124732, 2026.
Hou, G., Zheng, J., Cui, X., et al. Suitable coverage and slope guided by soil and water conservation can prevent non-point source pollution diffusion: A case study of grassland. *Ecotoxicology & Environmental Safety*, *241*, 113804. doi: 10.1016/j.ecoenv.2022.113804, 2022.
Huo, K., Shen, W., Wei, J., et al. Interpretable machine learning reveals the importance of geography and landscape arrangement for surface water quality across China. *Water Research*, *281*, 123578. doi: 10.1016/j.watres.2025.123578, 2025.
Krzeminska, D., Blankenberg, A.-G.B., Bechmann, M., et al. The effectiveness of sediment and phosphorus removal by a small constructed wetland in Norway: 18 years of monitoring and perspectives for the future. *Catena*, *223*, 106962. doi: 10.1016/j.catena.2023.106962, 2023.
Kumar Bhattacharya, R., Das Chatterjee, N., & Das, K. Linkages between gully erosion susceptibility and hydrological connectivity in Tropical sub-humid river basin: Application of Machine learning algorithms and Connectivity Index. *Catena*, *243*, 108186. doi: 10.1016/j.catena.2024.108186, 2024.
Lee, T.Y., Huang, J.C., Kao, S.J., et al. Temporal variation of nitrate and phosphate transport in headwater catchments: the hydrological controls and land use alteration. *Biogeosciences*, *10*(4), 2617-2632. doi: 10.5194/bg-10-2617-2013, 2013.
Lei, M., Shi, Y., Wang, J., et al. Rainstorms peak governs nitrate export pathways and patterns: Insights from high-frequency sampling and stable isotopes. *Water Research*, 125405. doi: 10.1016/j.watres.2026.125405, 2026.
Liu, G., Deng, L., Wu, R., et al. Determination of nitrogen and phosphorus fertilisation rates for tobacco based on economic response and nutrient concentrations in local stream water. *Agriculture, Ecosystems & Environment*, *304*, 107136. doi: 10.1016/j.agee.2020.107136, 2020.
Liu, X., Guo, M., Chen, Z., et al. Quantifying the contributions of precipitation, topography and human activity and their coupling to the development of permanent gully. *Geoderma*, *449*, 117015. doi: 10.1016/j.geoderma.2024.117015, 2024.
McDowell, R.W., & Haygarth, P.M. Reducing phosphorus losses from agricultural land to surface water. *Current Opinion in Biotechnology*, *89*, 103181. doi: 10.1016/j.copbio.2024.103181, 2024.
Miller, J.J., Curtis, T., Chanasyk, D.S., et al. Effectiveness of soil in vegetated buffers to retain nutrients and sediment transported by concentrated runoff through deep gullies. *Canadian Journal of Soil Science*, *96*(2), 154-168. doi: 10.1139/cjss-2015-0038, 2016.
Räty, M., Järvenranta, K., Saarijärvi, E., et al. Losses of phosphorus, nitrogen, dissolved organic carbon and soil from a small agricultural and forested catchment in east-central Finland. *Agriculture, Ecosystems & Environment*, *302*, 107075. doi: 10.1016/j.agee.2020.107075, 2020.
Risal, A., Parajuli, P.B., Dash, P., et al. Sensitivity of hydrology and water quality to variation in land use and land cover data. *Agricultural Water Management*, *241*, 106366. doi: 10.1016/j.agwat.2020.106366, 2020.
Ross, C.A., Moslenko, L.L., Biagi, K.M., et al. Total and dissolved phosphorus losses from agricultural headwater streams during extreme runoff events. *Science of the Total Environment*, *848*, 157736. doi: 10.1016/j.scitotenv.2022.157736, 2022.
Shi, Q., W., Wang, W., and Guo M. Headcut erosion characteristics revealed through simulated rainfall and scouring experiments in the gully region of the Loess Plateau. *Journal of Soil and Water Conservation*, *77(2)* 172-183. doi: 10.2489/jswc.2022.00152, 2022.
Su, L., Huang, D., Zhou, L., et al. Temporal sediment source tracing during storm events in the black soil region, Northeast China. *International Soil and Water Conservation Research*, *12*(2), 322-336. doi: 10.1016/j.iswcr.2023.07.005, 2024.
Sun, L., Liu, Y.-F., Wang, X., et al. Soil nutrient loss by gully erosion on sloping alpine steppe in the northern Qinghai-Tibetan Plateau. *Catena*, *208*, 105763. doi: 10.1016/j.catena.2021.105763, 2022.
Tang, J., Xie, Y., Wu, Y., et al. Influence of precipitation change and topography characteristics on the development of farmland gully in the black soil region of northeast China. *Catena*, *224*, 106999. doi: 10.1016/j.catena.2023.106999, 2023.
Walker, S.J., Wilkinson, S.N., & Hairsine, P.B. Advancing gully topographic threshold analysis using an automated algorithm and high-resolution topography. *Catena*, *239*, 107897. doi: 10.1016/j.catena.2024.107897, 2024.
Wang, J., Li, X., Li, Y., et al. Transport pathways of nitrate in stormwater runoff inferred from high-frequency sampling and stable water isotopes. *Environmental Science & Technology*, *58*(38), 17026-17035. doi: 10.1021/acs.est.4c02495, 2024.

Wang, L., Guo, M., Chen, Z., et al. Changes in soil TN and TP induced by freeze-thaw effect and the driving mechanism of environmental factors in a small watershed. *International Soil and Water Conservation Research*, 100609. doi: 10.1016/j.iswcr.2026.01.001, 2026.

Wang, R., Zhang, J., Cai, C., et al. How to control nitrogen and phosphorus loss during runoff process? – A case study at Fushi Reservoir in Anji County (China). *Ecological Indicators*, *155*, 111007. doi: 10.1016/j.ecolind.2023.111007, 2023.

Wang, T., Zhu, B., & Zhou, M. Ecological ditch system for nutrient removal of rural domestic sewage in the hilly area of the central Sichuan Basin, China. *Journal of Hydrology*, *570*, 839–849. doi: 10.1016/j.jhydrol.2019.01.034, 2019.

Wang, Y., Xu, H., Zhao, X., et al. Rainfall impacts on nonpoint nitrogen and phosphorus dynamics in an agricultural river in subtropical montane reservoir region of southeast China. *Journal of Environmental Sciences*, *149*, 551-563. doi: 10.1016/j.jes.2024.02.012, 2025.

Wenng, H., Bechmann, M., Krogstad, T., et al. Climate effects on land management and stream nitrogen concentrations in small agricultural catchments in Norway. *Ambio*, *49*(11), 1747-1758. 2020.

Winter, C., Tarasova, L., Lutz, S.R., et al. Explaining the Variability in High-Frequency Nitrate Export Patterns Using Long-Term Hydrological Event Classification. *Water Resources Research*, *58*(1), e2021WR030938. doi: 10.1029/2021wr030938, 2022.

Wu, J., He, S., & Lu, J. Multi-scale effects of topography and landscape pattern on riverine nitrogen and phosphorus nutrients in an agricultural watershed. *Landscape Ecology*, *40*, 112. doi: 10.1007/s10980-025-02131-y, 2025.

Xiao, M., Song, W., Zhang, H., et al. Eutrophication of Jiangsu coastal water and its role in the formation of green tide. *Journal of Ocean University of China*, *23*(1), 109-118. doi: 10.1007/s11802-024-5507-2, 2024.

Xu, J., Mo, Y., Tang, H., et al. Distribution, transfer process and influence factors of phosphorus at sediment-water interface in the Huaihe River. *Journal of Hydrology*, *612*, 128079. doi: 10.1016/j.jhydrol.2022.128079, 2022.

Xu, L., Lu, J., & Zhang, D. Assessing impacts of rainfall intensity and slope gradient on runoff process and dissolved organic carbon loss via surface flow and interflow under simulated rainfall. *PLoS One*, *21*(1), e0328611. doi: 10.1371/journal.pone.0328611, 2026.

Yang, C., Hu, Y., Li, Z., et al. Relating rainfall, runoff, and sediment to phosphorus loss in northern rocky mountainous area of China. *Catena*, *247*, 108504. doi: 10.1016/j.catena.2024.108504, 2024.

Zhang, G., Xu, T., Song, J., et al. Characterization of runoff phosphorus loss from a combination of long-term fertilizer application and cultivation on sloping croplands. *Journal of Hydrology: Regional Studies*, *54*, 101907. doi: 10.1016/j.ejrh.2024.101907, 2024.

Zhang, Q., Xu, H., & Zhang, Z. Plot size modulates the effects of vegetation on soil and water conservation at the slope scale on China's Loess Plateau. *Catena*, *258*. doi: 10.1016/j.catena.2025.109284, 2025.

Zhang, S., and Zhang, K. Assessing the impact of extreme rainfall and slope surface conditions on runoff and erosion based on a big database in Southwest China's karst region. *Journal of Hydrology*, *659*(659), 133273. doi: 10.1016/j.jhydrol.2025.133273, 2025.

Zhang, Z., Kong, L., Zhu, L., et al. Fate characteristics of nitrogen in runoff from a small agricultural watershed on the south of Huaihe River in China. *Environmental Earth Sciences*, *66*(3), 835-848. doi: 10.1007/s12665-011-1293-4, 2011.

Zhao, H., Liu, X., Du, X., et al. Impacts of storm events on watershed phosphorus critical source area identification based on SWAT model. *Journal of Hydrology*, *668*, 135032. doi: 10.1016/j.jhydrol.2026.135032, 2026.

Zhao, L., Fu, D., Li, T., et al. Temporal variations of N and P losses via surface runoff from Chinese farmland after fertilisation. *Soil and Tillage Research*, *246*, 106338. doi: 10.1016/j.still.2024.106338, 2025.